Hindawi
Journal of Advanced Transportation
Volume 2023, Article ID 5583901, 14 pages
https://doi.org/10.1155/2023/5583901

Research Article

Automated Lane-Level Road Geometry Estimation Using Microscopic Trajectory Data

Junhua Wang,[1] **Chengmin Li**,[1] **Ting Fu**,[1] **Lanfang Zhang**,[1] **Anae Sobhani**,[2] **and Jiangtian Xue**[1]

[1]*The Key Laboratory of Road and Traffic Engineering, Ministry of Education, Tongji University, Shanghai, China*
[2]*Barney School of Business, University of Hartford, West Hartford, USA*

Correspondence should be addressed to Lanfang Zhang; zlf2276@163.com

Received 21 July 2023; Revised 26 November 2023; Accepted 27 November 2023; Published 11 December 2023

Academic Editor: Zhihong Yao

Vehicle trajectory data is in high demand for transportation research due to its rich detail. Lane information is an important aspect of trajectory data, which is typically obtained using sensors such as cameras or LiDAR, which are able to extract road lane features. However, some sensors for trajectory tracking (e.g., MMW radar sensors) are unable to provide lane information. Vehicle detection and trajectory tracking systems based on these sensing technologies can integrate with lane information through manual calibration during initial installation, but this process is labor-intensive and requires frequent recalibration as the sensors gradually become deviated by wind and vibration. This has posed a challenge for trajectory tracking, particularly for real-time applications. To address this challenge, this paper proposes a method for estimating lane-level road geometrics using microscopic trajectory data. The method involves segmenting the trajectory points using direction vectors and clustering them and fitting a series of cluster center points. The mean error (ME) of the distance between the estimated result and the ground truth reference is used to measure the accuracy of the lane-level road geometrics estimation in different conditions. Results show that when the average trajectory data includes at least approximately 30 points per meter in each segment, the ME is always less than 0.1 m. The method has also been tested on MMW wave radar data and found to be effective. This demonstrates the feasibility of our approach for dynamic calibration of road alignment in vehicle trajectory tracking systems.

1. Introduction

Vehicle trajectory data are a valuable resource in the field of transportation, and there has been a proliferation of research on topics such as road safety, microdriving behavior, and autonomous driving using trajectory data acquired through various sensing technologies, including computer vision [1, 2], radar [3, 4], and LiDAR [5, 6]. Vision-based tracking is the most commonly used method for extracting trajectories, as seen in datasets such as the Next Generation Simulation (NGSIM) [7] which uses video data from cameras mounted on tall buildings, and the highD dataset [8], which uses unmanned aerial vehicles (UAVs) to collect data from above the roads. MMW radar, which extracts trajectories using the Doppler effect of waves, has also been shown to be effective for trajectory extraction [3] and has been applied to a wide range of scenarios [9]. LiDAR, on the other hand, provides rich, detailed trajectory data and has been used in numerous experimental studies [5, 6].

Despite advances in trajectory extraction techniques, a crucial question remains: how can we accurately obtain geometric information for further analysis? Road geometric information is important at the microscopic behavior level, as lateral maneuver information such as lateral offsets and accelerations is a key aspect of behavior and related road user safety [10]. In addition, the current trend of sensor fusion (both trajectory splicing and data fusion) also requires proper identification of lane information [11]. It is worth noting that the road geometry mentioned in this paper refers specifically to features such as curves and lanes on the plane and does not include longitudinal sections. Because

trajectory extraction is typically carried out on expressways or urban expressways, which tend to be relatively smooth.

There are two main approaches for obtaining geometric information from vehicle data: the direct detection approach, in which geometrics are directly detected using sensors such as cameras and LiDAR, and the indirect estimation approach, which estimates geometric information based on vehicle trajectory data collected by sensors such as MMW radars. For example, the highD dataset [8] manually obtained geometric information from clear lane lines in UAV images, which can even provide complex geometry information for interwoven regions where highways enter and exit [12]. LiDAR can also provide point cloud data containing road information for geometric information extraction [13]. MMW radars, which offer better tracking capability and speed accuracy compared to video cameras [14], have gained increasing popularity for real-time traffic data collection [3]; for these sensors, as geometric information cannot be directly recorded, studies have attempted to estimate geometric information from extracted trajectories. For instance, roadside MMW radar can extract road information through trajectory clustering and fitting [15].

Despite the efforts made in obtaining geometric information, current methods have their limitations. Direct methods, such as deep learning or image processing using images or LiDAR point clouds, are often complex and can result in slow processing times. These methods may also not be applicable in all scenarios, such as at night or in low visibility, and often require clear lane lines for accurate results [16, 17]. Indirect methods, which rely on the accuracy of trajectory data [18], can provide some level of accuracy [15], but the range of geometric information obtained is usually limited [15, 18] and may require supplementary information for completeness [19]. Additionally, sensor fusion technology, which combines multiple sensors to improve accuracy, can be expensive due to the need for periodic recalibration and can be affected by offsets caused by wind and vibration. In order to obtain high quality data, these sensors must be continuously calibrated.

This study aims to develop a method for estimating lane-level road geometry using trajectory data. To do so, we used existing datasets for experimentation and validated the ground truth reference acquired from these datasets using manually calibrated data from UAVs. We then presented a method for segmenting and clustering trajectory data to generate a series of points, which were used to estimate lane-level geometry after undergoing polynomial fitting and smoothing. We conducted a case study using UAV trajectory data to validate the method and compared the results under different conditions, including the presence or absence of lane change vehicle trajectories, different amounts of data, different lengths of trajectory segmentation, and different clustering methods. Finally, we applied the method to MMW radar data in a case study, demonstrating its effectiveness in calibrating lane estimation in existing radar systems and other sensors that do not provide lane information.

2. Literature Review

Lane-level road geometrics have been widely studied in the context of autonomous driving and advanced driver assistance system [20]. The purpose of identifying lane lines is to construct a driving scene and to determine the driving environment [21]. Most existing studies on lane detection using on-board equipment have focused on extracting lane lines from image features through camera-based methods [17] or point cloud features through LiDAR-based methods [22]. Eidehall et al. [19] demonstrated that combing the trajectory data with road information can improve the accuracy of lane detection. Zhang [18] further showed that road shape can be successfully estimated solely based on trajectory data. It is worth noting that although direct detection and indirect estimation methods are different, their accuracies are similar. For roadside sensors, information in a fixed area can be acquired over a long period of time. Cameras are a commonly used solution as they can acquire target images effectively. Meanwhile, LiDAR provides a high-precision advantage with its ability to gather three-dimensional point cloud data [23]. Both LiDAR and cameras can directly obtain lane lines through data features. While millimeter-wave radar cannot directly provide lane line information, it is generally less expensive than LiDAR and is increasingly being used for roadside traffic detection [4, 9]. Some studies have reported that millimeter-wave radar combined with other sensors (primarily cameras) as a fusion sensor is reliable [24, 25]. To the best of the author's knowledge, there has been very little research directly investigating road geometrics using trajectory data. Wang et al. [9] presented a real-time road-range tracking of vehicle trajectories using millimeter-wave radar sensors, in which trajectory splicing (combining the trajectory data of adjacent areas to obtain the trajectory data of a larger area [26]) is necessary. However, some work relies on a multicamera tracking system and the road geometry is obtained through image processing [27]. With road geometry, the spatial relationship of vehicles can be more easily aligned across different sensors. Wang et al. [9] mentioned that road geometry can also be accurately estimated from high-precision trajectory data in pure millimeter-wave radar systems.

In both direct detection and indirect estimation methods, despite the variations in approaches, the representation of road geometry is consistent in most studies. Previous studies have shown that road geometry is commonly described in a flat 2D plane as an assumption [20]. There are three types of models that can be used to fit road geometry: parametric, semiparametric, and nonparametric. Zhang [18] suggested that a polynomial model is effective in describing road geometry with few parameters. Li et al. [28] also found that the least-squares method is effective in fitting lane lines. However, it is worth noting that the alignment of a road consists of various types of lines, and it can be difficult to fit sharp changes in the road using a single model when the fitting section is too long [29]. Feature points used in the fitting process include lane line feature points [20] and roadside object [30]. It is worth noting that most of the studies still require real environmental data.

While past literature has not extensively explored the use of trajectory data for lane-level road geometry detection, researchers have recognized the potential of this data for estimating road geometry. Liu and Sun [31] found that the wheel rails of vehicles have different distributions in different lanes in the cross section of the road, although the exact distribution cannot be accurately expressed due to the limitations of the data. Huang and Jianchuan [32] also discovered that different types of vehicles have distinct distributions in the road cross section, with larger vehicles having a center value of their lateral trajectory distribution that is closer to the center line of the lane. While there have been fewer studies on using trajectory data to detect road alignment, there have been numerous studies on using trajectory data to evaluate driving characteristics under different road alignment conditions [33, 34].

Therefore, previous studies have demonstrated that trajectory data can be used to express road alignment. This research aims to address the gap in the use of microscopic trajectory data, specifically roadside equipment collection trajectory data, for estimating lane-level road geometry. Even if there is a sensor offset, road information can still be estimated through the trajectory data by dynamically calibrating road alignments for vehicle trajectory tracking systems.

3. Methodology

The methodology for this research is outlined in Figure 1. It consists of three main steps: (i) data collection and ground truth reference acquisition, (ii) trajectory clustering and estimation, and (iii) comparison and application.

3.1. Data Collection and Ground Truth Reference Acquisition. The NGSIM dataset is widely used in transport research and consists of trajectory data derived from video. While these datasets do not provide road alignment or lane line information, they can be used as a reference for comparison of estimation results. To obtain ground truth reference for each lane center line, we used the method proposed by Zhang [18] of fitting all in-lane trajectories with a smoothing spline function using a third-degree polynomial model. It is worth noting that this method is only suitable for road sections without complex facilities, such as bus stops and entry and exit ramps, or road sections with drastic changes in cross-section.

To acquire the ground truth reference for each lane center line, we first eliminated interference items from the trajectory data, such as lanes affected by ramps in the NGSIM data, which were labeled as the 6th and 7th lanes. In this research, we removed the trajectory data for lanes 6 and 7, following Zhang's approach. Next, we fit all in-lane trajectories with a third-degree polynomial model using the least squares method in the global coordinate frame. These samples were then treated as the ground truth reference for the lane lines in the global coordinate frame and served as a reference for each lane, as shown in Figure 2. However, since the NGSIM data does not have lane line information, it is impossible to verify the reliability of this method. To test the results, we manually annotated the lane center lines using UAV video, which can be used as validation of the method. Specifically, we marked feature points on each lane line manually, and then fit these points with a third-degree polynomial model using the least squares method. The calibrated lane center line was then obtained by averaging the models of the nearest lane lines.

In the UAV video, the vehicle trajectory data were also manually calibrated. Considering the need to study the impact of different data volumes on clustering methods, the current hovering time of drones is generally limited, which makes it difficult to provide continuous long-term trajectory data. Additionally, manual calibration is time-consuming, so we used the previous ground truth reference estimation method as a supplement after validation [18], if a large amount of data was needed. Note that throughout this paper, the term "ground truth reference" does not refer to the true value, but rather serves as a reference value for lane estimation. The manually annotated value obtained from the UAV is referred to as the ground truth lane center line in this research.

3.2. Trajectory Clustering and Lane Estimation. Sensors such as MMW radar can detect vehicle trajectories without initially recording their lane information. In the NGSIM I80 dataset, we can infer the lane information of a vehicle through the video. Therefore, in the processing process, we need to remove the label indicating the lane ID that the vehicle is on. To obtain lane change information, we use a polynomial fitting on each vehicle trajectory to remove lane change data. This results in pure discrete points with only time and position, which can be treated as the pure trajectory of a sensor that does not provide lane information. The UAV trajectory data are also processed in this way.

Since pure trajectory data does not provide lane direction and road geometry is not a straight line, it is impossible to capture lane-level geometry in road latitude and longitude. To approximate the lane direction, we randomly select the start and end points of a vehicle's trajectory to represent a direction vector. This selection is used only to confirm the approximate direction, and the normal vector perpendicular to the direction vector is divided equally, as shown in Figure 3(a). The blue dashed line is called the divide line, which produces a block area. Each lane ID is then obtained by clustering as shown in Figure 3(b). The edges of the lanes are not shown in these figures because this is pure track data.

For lateral clustering, we prepare the trajectory segment and start clustering according to Figure 3(c) to obtain the segment cluster center of each lane on the entire road (representing the cross-section center point of each lane). To avoid local optima, we delete any data sets where the cluster centers for different segments are too close or unreasonable. This step is repeated for each segment, resulting in a sequence of discrete points. Finally, by fitting these points (cleaned segment clustering centers) with a third-degree polynomial model using least squares, we can obtain the

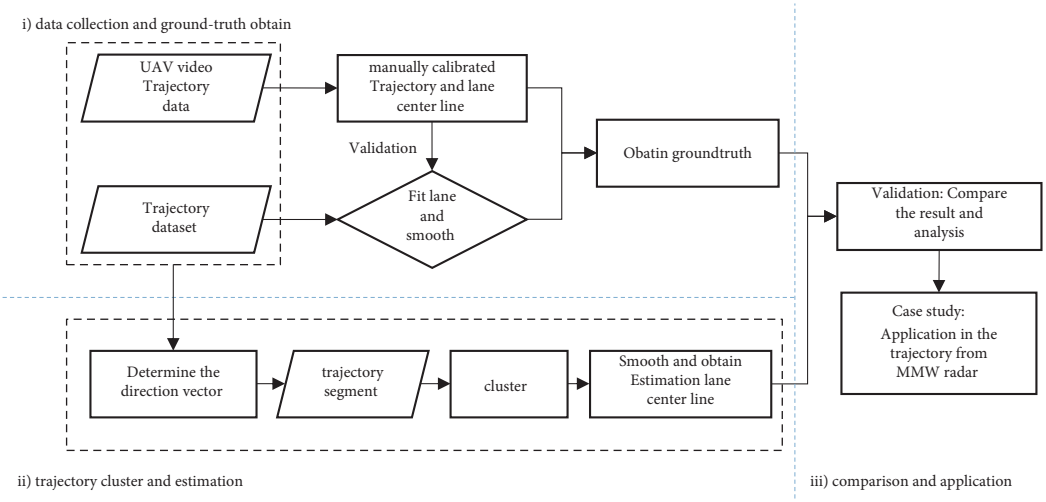

Figure 1: Methodology flowchart.

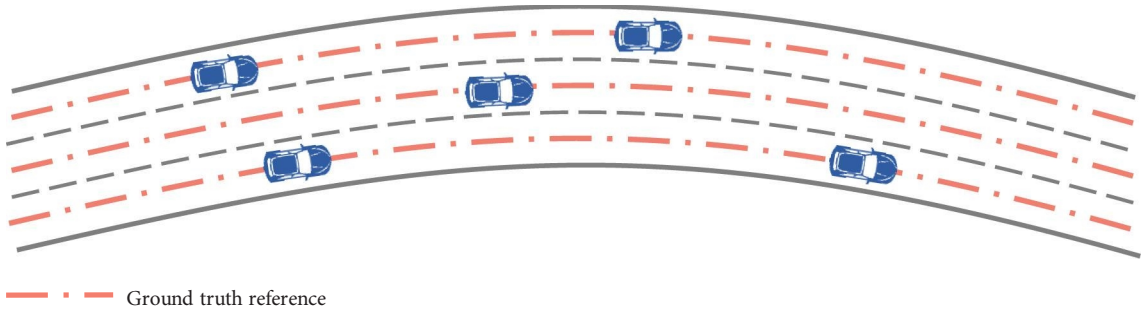

Figure 2: Illustration of ground truth reference data.

estimation of the lane center line as the black curved line as shown in Figure 3.

For a trajectory segment, the vehicle's trajectory points can be thought of as a random variable input, similar to the problem of an archer shooting a target. This includes an assumption that the lateral distribution of trajectories on each lane follows a normal distribution, meaning that the sample mean can be used to represent the distribution mean, which is at the centerline of the lane. However, this assumption is only used in the lane cross-section, and the coordinate system of this dataset does not align with the cross-section. As shown in Figure 4, the segment centers represent the center point of the cross-section after the clustering is completed and can be represented by the center of all the trajectory points in that segment. Using these cluster centers as lane feature points, we can estimate the lane center line. The process for doing so will be demonstrated in formulas (1)–(6). Details are explained in the following part.

A cluster of trajectory data segment is presented in Figure 4. The midpoint of the projection of all trajectory points on the cross-section, represented by (x', y'), is used as the center point of the segment. The value of y' can be calculated using the following equation, and the value of x' can be similarly determined:

$$y' = \frac{\sum_i^N [y_i - d_i \sin \boldsymbol{\theta}]}{N} = \frac{\sum_i^N y_i}{N} - \frac{\sum_i^N d_i \sin \boldsymbol{\theta}}{N}, \tag{1}$$

where d_i represents the distance between the trajectory point i and the red line (cross-section line) and $\boldsymbol{\theta}$ represents the angle between the x-axis and the d_i of the point, measured clockwise. N is the number of trajectory segment points. In addition, the center of all trajectory points is (x'', y''), and y'' can be calculated based on the following equation. Similarly, x'' is not listed anymore either.

$$y'' = \frac{\sum_i^N y_i}{N}. \tag{2}$$

The center point of the cross-section can be represented by the mean of the trajectory segments only if $(x', y') = (x'', y'')$ are equal, which can be verified using the following equation:

$$\frac{\sum_i^N d_i \sin \boldsymbol{\theta}}{N} = 0. \tag{3}$$

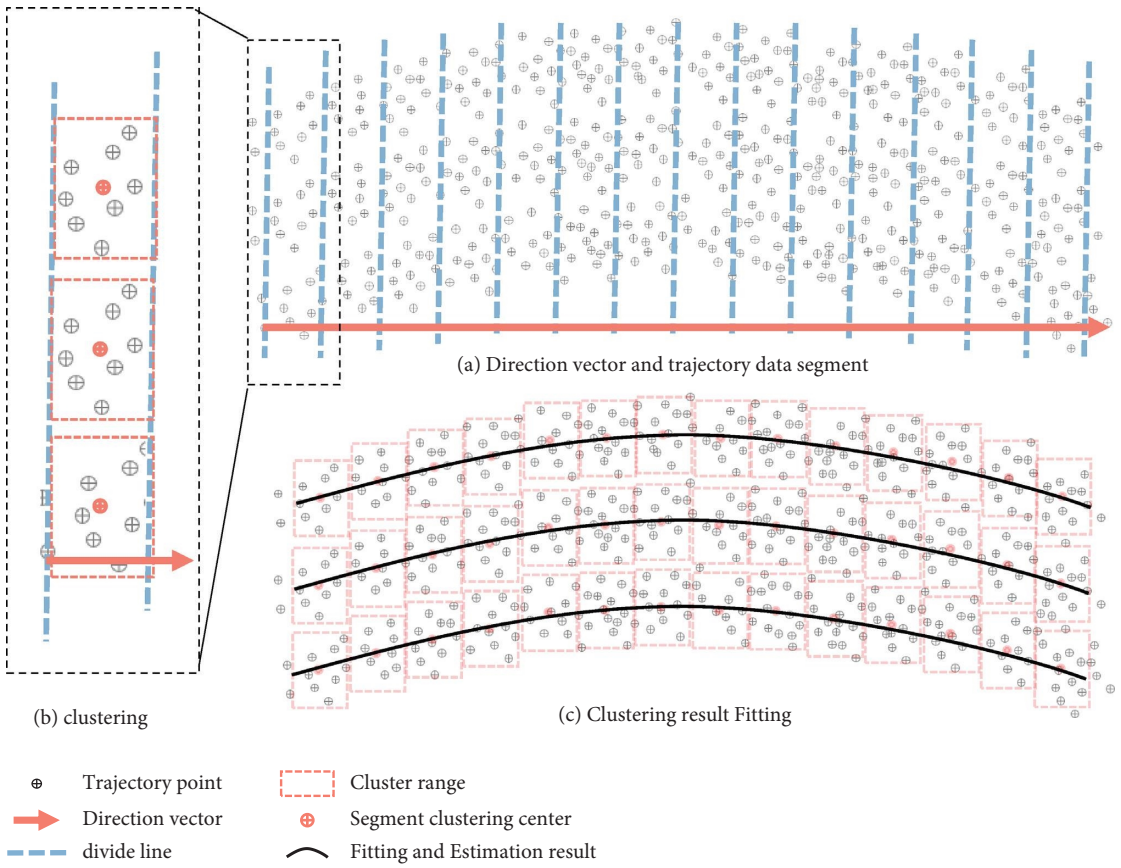

Figure 3: Process of the lane-level geometry estimation method.

The cross-section line equation is given as $Ax + By + C = 0$, where A, B, and C are all constants. This line should be perpendicular to the edge line. The distances can be calculated, and equation (3) can be rewritten as the following equations:

$$\sum_{i}^{N} Ax_i + By_i + C = 0, \tag{4}$$

$$A\sum_{i}^{N} x_i + B\sum_{i}^{N} y_i + N \times C = 0, \tag{5}$$

$$Ax'' + By'' + C = 0. \tag{6}$$

This suggests that if the cross-section line equation passes through the points (x'', y''), it will satisfy equation (3). In other words, the center of all trajectory points (x'', y'') can represent the segment center (x', y') on the cross section.

In this study, we used two clustering methods: the commonly used *K*-means method and the k-medoids method, which uses actual points in the class as the center instead of the mean center to reduce error caused by outliers. It should be noted that the *k*-values of these two methods are consistent with the actual number of lanes. For instance, if trajectory data is collected on a 3-lane road, we select the *k*-value as 3, and so forth. The length of the segment affects the number and accuracy of the clusters directly. To ensure that each segment contains at least one point, we considered the speed of the vehicle. For example, if the data frequency is more than 10 Hz and the average speed of the road is 20 m/s, the segment length should be more than 2 m. We compared the clustering effect under different segmentation lengths.

Another issue we had to address was the presence of "jagged" edges at the start and end of the radar detection range, where vehicles are not detected at the same position, resulting in abnormal clustering. To fix this, we trimmed the start and end of the trajectory range. With these preparations, the trajectory clustering is essentially completed.

3.3. Comparison and Application. The final estimation result is measured using the average distance between the curves as the error, as shown in Figure 5. Specifically, we calculate the difference between the estimated value and the true value curve at certain points along the length by finding the closest distance from each point to the true value and then take the average to get the error of the entire curve. When measuring all lanes, we take the average of the mean error (ME) for different lanes; ME can be calculated using the following equation:

$$\mathrm{ME} = \frac{\sum(d1, d2, \ldots, dn)}{n}. \tag{7}$$

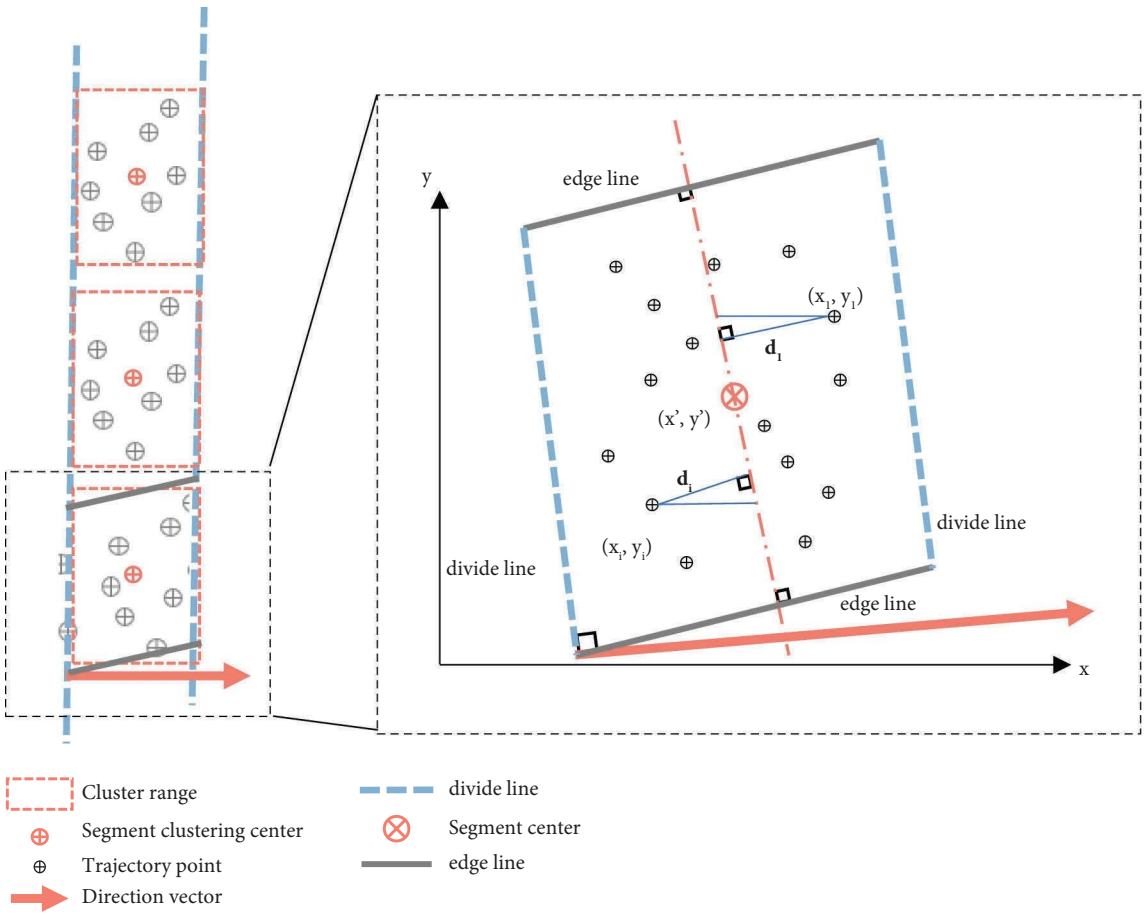

Figure 4: A cluster in the trajectory data segment. *Note that the edge line is the edge of a lane, the red dash-dot line is the road cross section perpendicular to the edge line, and the blue dashed line is perpendicular to the direction vector and serves as the divide line. The zoomed figure is slightly skewed for ease of presentation.

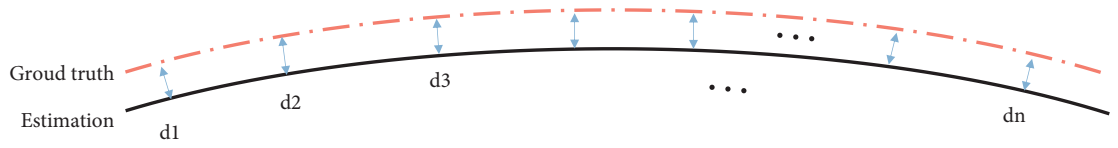

Figure 5: Distance between the estimated and ground truth curves.

To analyze the effects of various experimental conditions on the estimated results, we repeat the above process for the NGSIM datasets using different segment lengths, clustering methods, and data amounts and with or without lane change data. The parameters with the best results are selected and then verified with the manually calibrated data. Finally, the method with the selected parameters is applied to the trajectory data from the MMW radar. Since the radar data does not have real lane line data, we also use the ME of two adjacent geometric estimation results for evaluation.

4. Validation

4.1. Site and Data for Validation. In this paper, two datasets were used to evaluate the proposed method for estimating lane-level road geometry using microscopic trajectory data. The first dataset, NGSIM, open-sourced, contains a large number of microscopic trajectory data points, while the second dataset consists of a relatively small amount of manually calibrated UAV trajectory data. The UAV data were used as a validation method to assess the effectiveness of the ground truth reference method of the NGSIM data. The lane-level road geometry estimation results of the two datasets were then compared under different conditions, including different segment lengths, the inclusion or exclusion of lane-changing values, and different amounts of data.

4.1.1. Description of the NGSIM Datasets. The NGSIM datasets used in this research were extracted from video images taken by cameras mounted on top of buildings, as shown in Figure 6 [7]. The study site, located on I-80, is approximately 500 meters in length and has 6 lanes, with the

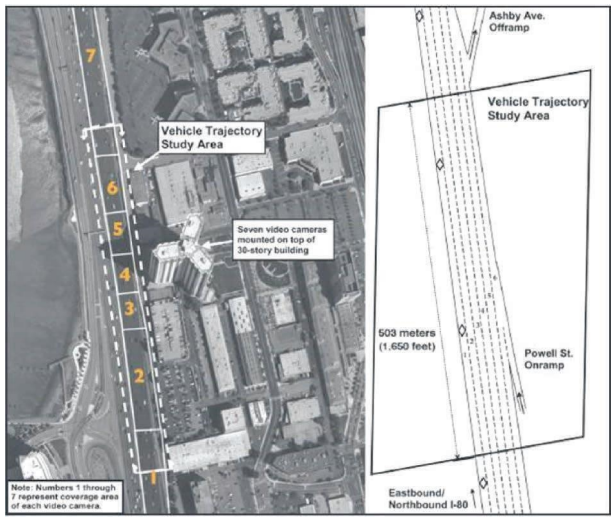

Figure 6: Description of the NGSIM I-80 dataset [7].

6th lane merging with an entrance ramp, and the ramp is number 7 lane in the dataset. To eliminate the influence of vehicle trajectories at the ramp, the trajectories in the 6th and 7th lanes were removed from the analysis. The data were collected at a frequency of 10 Hz during two time periods: 15 minutes from 4:00 p.m. to 4:15 p.m. and 30 minutes from 5:00 p.m. to 5:30 p.m. on April 13, 2005.

4.1.2. Description of Hangzhou Xifu Freeway Dataset. The second dataset used in this research was collected using a DJI Mavic2 Prounmanned aerial vehicle (UAV) on the Hangzhou Xifu Freeway, as shown in Figure 7. The UAV flew above the road section for a duration of 8 minutes, recording video of the traffic with a resolution of $3840 * 2160$. The captured road section was approximately 190 meters in length, and the video provided clear enough lane line markings for calibrating the lane center line.

4.2. Analysis and Discussions

4.2.1. Ground Truth Reference Acquisition Method Validation. The results of the lane center line calibration are shown in Figure 8. As shown in Figure 8(a), the red line fits the lane lines well, and the mean of the two-lane lines (blue line) also fits well. The comparison between the lane center line and the ground truth reference is shown in Figure 8(b). It should be noted that the ground truth was obtained by fitting the trajectory data after removing the lane change data, and it serves as a reference. The ME of the fitting model is 0.087 in lane 1, 0.035 in lane 2, and 0.160 in lane 3, as shown in Figure 8(c). The average ME is below 0.1 meters, which is less than 2.6% of the lane width of 3.75 meters in this study. However, it is ambiguous whether these results prove the high accuracy of this method. The purpose of this validation experiment was to demonstrate that this method is relatively effective, and the ground truth of the NGSIM I-80 datasets will be estimated using this method as a reference, as shown in Figure 9.

4.2.2. Lane-Level Road Geometrics Estimation. To investigate the effect of different segment lengths, clustering methods, inclusion or exclusion of lane-changing values, and different amounts of data on the lane-level geometry estimation, the estimation results were analyzed under different conditions. The results are shown in the following figures and tables.

(1) NGSIM Dataset. As can be seen in Figure 10, four groups of control experiments were carried out, respectively. k is a simple k-means method, km is a simple k-medoids method, ku and kmu mean corresponding methods after lane change data are removed, as the amount of data increases, and the ME of all the results gradually decreases. From the figure, it appears that the performance is better when the lane change data is removed, especially for high amounts of data. However, for low amounts of data, the performance is worse without the lane change data. Using the k-medoids method for clustering can also effectively improve the results for large amounts of data, but the fitting effect is not as good as the k-means method for small amounts of data. This may be because the k-medoids method is less sensitive to anomalous data for large amounts of data. It is worth noting that all the data points in the figure are the mean values obtained from multiple experiments. The large difference when the amount of data is small is mainly due to the fact that, in this experiment, the lane change data was completely removed, not just part of the trajectory, resulting in significantly different data used for analysis (in actual operation, it is usually easier to remove the entire lane change trajectory rather than just a part of it).

Results related to lane analysis are presented in Table 1 and Figure 11. Based on the results of the estimation using a 1-meter segment length, the ME differs between lanes. One interesting aspect of the data shown in this figure is that the errors for lanes 1 and 2 are relatively small, the errors for lane 3 are in the middle, and the errors for lanes 4 and 5 are relatively high. This may be due to the different lateral distribution characteristics of vehicles in different lanes and the fact that lanes 4 and 5 are relatively close to the ramp. When the amount of data is large, the accuracy of lane 2 is higher than that of lane 1, which may be due to the fact that the vehicle velocity on lane 1 is faster and the majority of vehicles are cars, resulting in larger lateral deviation from the center line [31].

Results related to segment length are presented in Table 2 and Figure 12. This part of the experiment uses k-medoids method. From the figure and table, it can be clearly seen that when the cutting length is higher than 5 m, the accuracy decreases significantly, and when the cutting length is less than 4 m, the accuracy is still high. This is because the segmentation length determines the clustering area will be too long and the clustering will fall into a local solution. In addition, the width of the lane is around 3.75 m. Overall, while the segment length is less than 4 m, length did not affect the fit result accuracy; the final fitting accuracy can still be around 0.05. When the amount of data exceeds 100,000, it can be seen that the accuracy of the result of experiment length below 4 m has reached 0.1 m. From Table 2, when the data amount reaches 80000, as indicated by the boled row in the table, the NGSIM road involved is approximately 500 meters length

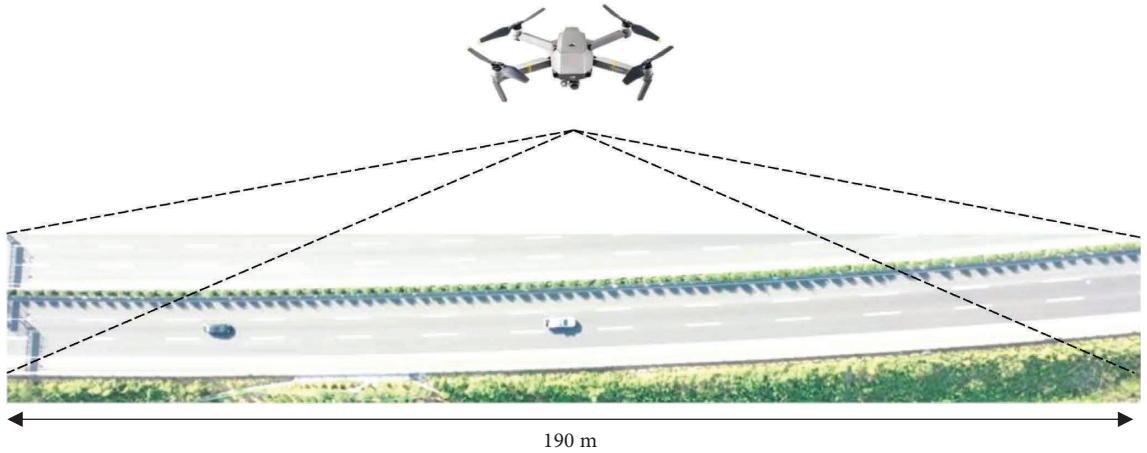

Figure 7: Data collection for the UAV video.

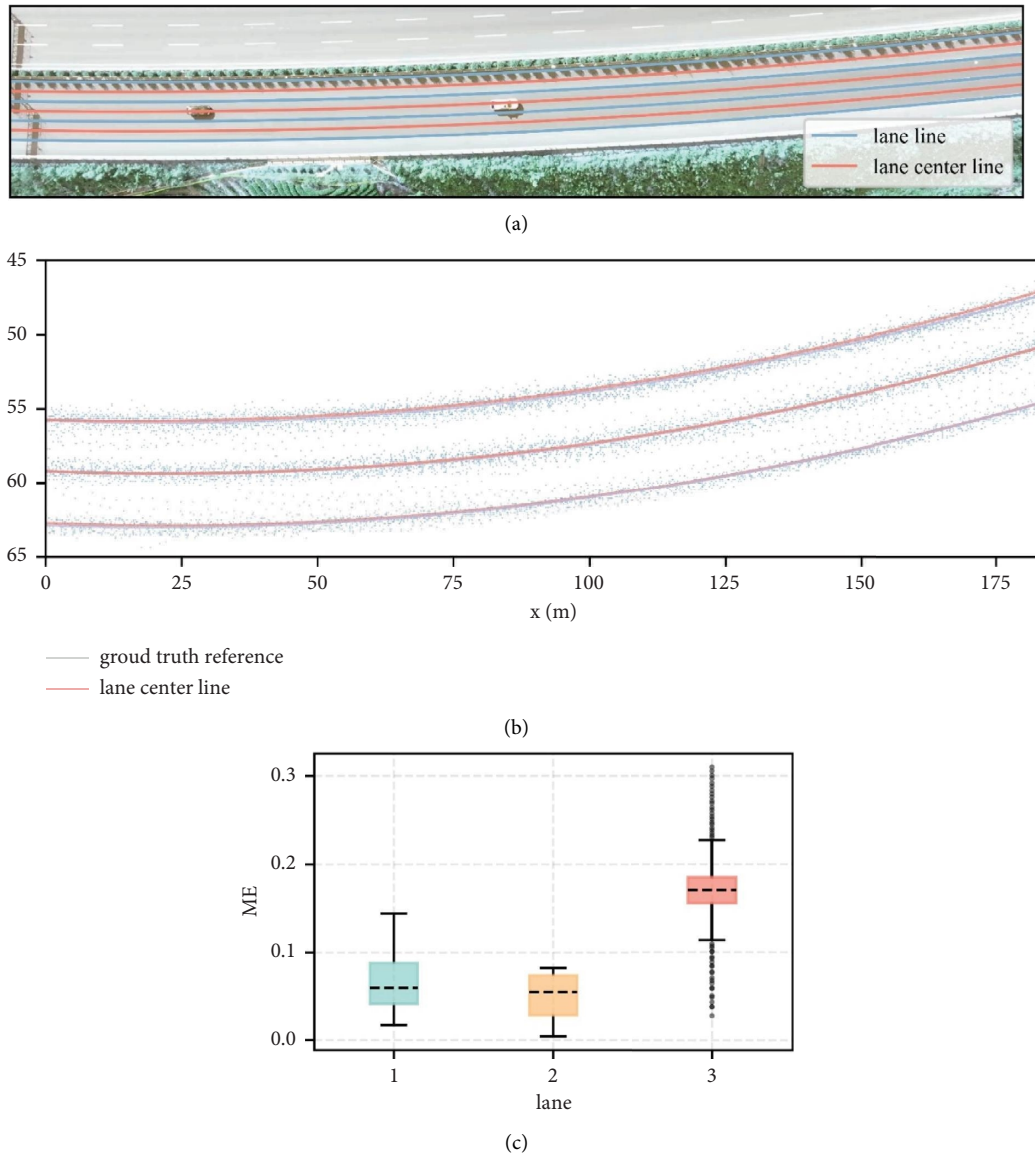

Figure 8: UAV video calibration result. (a) Lane line and lane center line calibration result. (b) Lane center line and ground truth reference. (c) Lane center line and ground truth reference error boxplot.

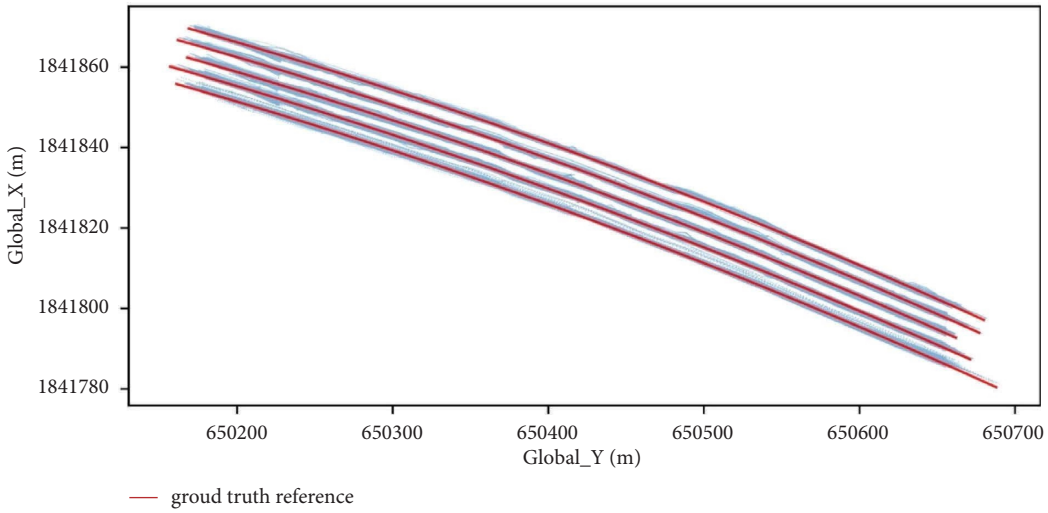

Figure 9: The ground truth reference of NGSIM I-80.

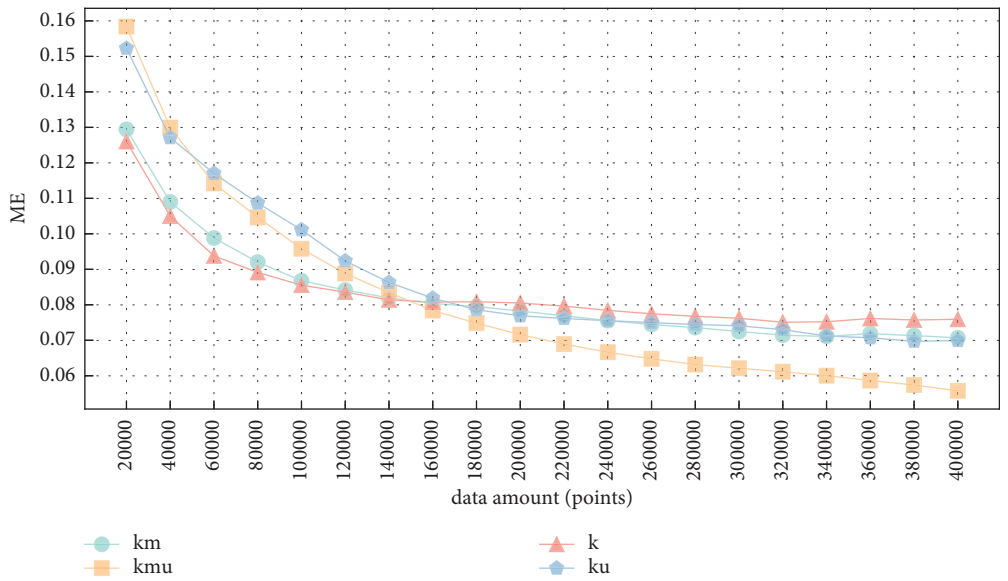

Figure 10: The estimation result in the different clustering methods.

with 5 lanesone can further prove that the accuracy is about 0.1 m, with a average of about 30 points one lane per meter (obtained by dividing 80000 by 500 and then by 5).

(2) UAV Manually Calibrated Trajectory Data. From the data extraction results, there are a total of 11152 trajectory points in the calibrated data from the UAV (of which only 3 are lane-changing vehicle data). The *k*-means method was chosen for clustering, with a segmentation length of 3 m. Figure 13 and Table 3 show the error between the ground truth reference and the estimation result, with an average ME of 0.018. Our method involves returning lane labels through clustering, with subsequent fitting that is approximately equivalent. The table also shows that the ME of the estimation result and lane center for lane 1 is 0.064, for lane 2, it is 0.067, and for lane 3, it is 0.182. The average ME is also below 0.1 m.

Based on the validation representing minimal differences between ground truth reference and lane center lane, the estimation results tended to be consistent with the ground truth reference. This was primarily due to that the ground truth reference and the estimation result are both based on the same trajectory data. Consequently, both the estimated results and the ground truth reference exhibited a larger fitting error in the third lane compared to the other two lanes. This could be attributed to the greater distance of the center line of the third lane's vehicle distribution from the lane center, which aligns with the results from the previous NGSIM comparative analysis across different lanes.

5. Case Study

While some of the trajectory datasets mentioned above provide a stable basis for significant research on traffic safety

Table 1: The estimation result in each lane.

Data amount	The ME/(m) of each line					Average ME
	Lane 1	Lane 2	Lane 3	Lane 4	Lane 5	
20000	0.141	0.136	0.187	0.160	0.167	0.158
40000	0.109	0.118	0.158	0.130	0.136	0.130
60000	0.095	0.105	0.132	0.114	0.125	0.114
80000	0.086	0.096	0.118	0.108	0.115	0.105
100000	0.081	0.086	0.108	0.098	0.106	0.096
120000	0.076	0.079	0.100	0.090	0.100	0.089
140000	0.073	0.072	0.093	0.084	0.096	0.083
160000	0.068	0.066	0.087	0.079	0.092	0.078
180000	0.062	0.062	0.082	0.078	0.090	0.075
200000	0.057	0.058	0.076	0.078	0.089	0.072
220000	0.053	0.053	0.072	0.079	0.088	0.069
240000	0.049	0.048	0.069	0.080	0.088	0.067
260000	0.048	0.043	0.066	0.079	0.087	0.065
280000	0.048	0.039	0.064	0.078	0.087	0.063
300000	0.047	0.037	0.062	0.077	0.086	0.062
320000	0.046	0.036	0.062	0.075	0.086	0.061
340000	0.047	0.034	0.060	0.074	0.085	0.060
360000	0.046	0.032	0.058	0.072	0.085	0.059
380000	0.046	0.031	0.056	0.070	0.083	0.057
400000	0.046	0.030	0.053	0.068	0.082	0.056

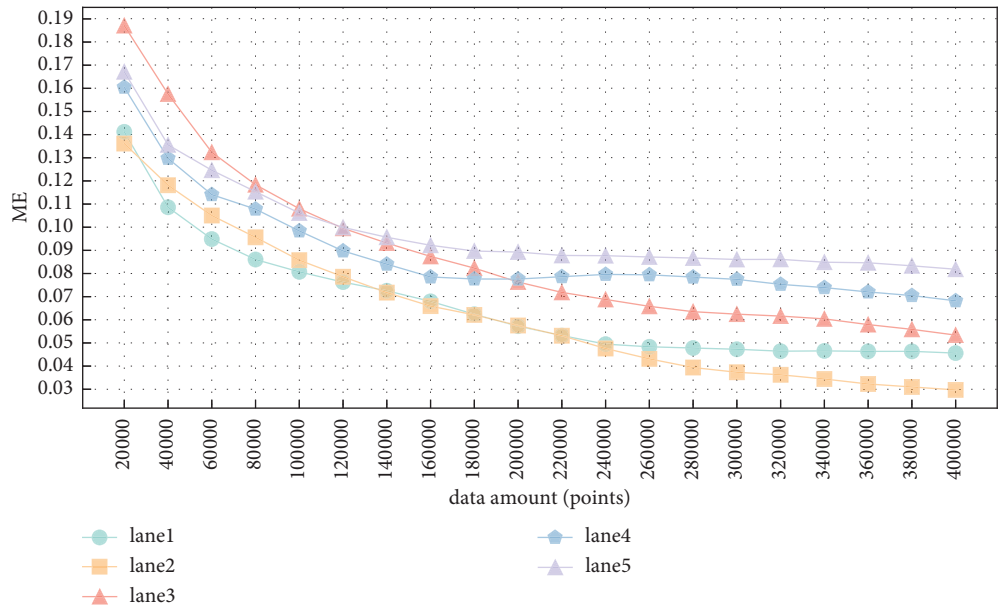

Figure 11: The estimation result in each lane.

Table 2: The estimation results for segments with different lengths.

Data amount	The ME/(m) of each segment length					
	1 m	2 m	3 m	4 m	5 m	6 m
20000	0.158	0.159	0.160	0.262	0.391	0.571
40000	0.130	0.131	0.133	0.161	0.242	0.401
60000	0.114	0.114	0.113	0.126	0.191	0.305
80000	**0.105**	**0.104**	**0.103**	**0.104**	0.132	0.274
100000	**0.096**	**0.094**	**0.095**	**0.102**	0.139	0.254
120000	0.089	0.087	0.088	0.093	0.118	0.240
140000	0.083	0.082	0.080	0.084	0.097	0.231
160000	0.078	0.077	0.077	0.081	0.105	0.197

Table 2: Continued.

Data amount	The ME/(m) of each segment length					
	1 m	2 m	3 m	4 m	5 m	6 m
180000	0.075	0.073	0.073	0.077	0.095	0.174
200000	0.072	0.069	0.069	0.071	0.090	0.176
220000	0.069	0.067	0.067	0.071	0.083	0.174
240000	0.067	0.066	0.064	0.069	0.088	0.152
260000	0.065	0.064	0.064	0.066	0.080	0.152
280000	0.063	0.063	0.061	0.066	0.076	0.166
300000	0.062	0.061	0.059	0.065	0.073	0.146
320000	0.061	0.060	0.058	0.060	0.079	0.145
340000	0.060	0.059	0.059	0.062	0.070	0.131
360000	0.059	0.057	0.056	0.057	0.076	0.157
380000	0.057	0.057	0.053	0.058	0.072	0.158
400000	0.056	0.055	0.052	0.060	0.073	0.133

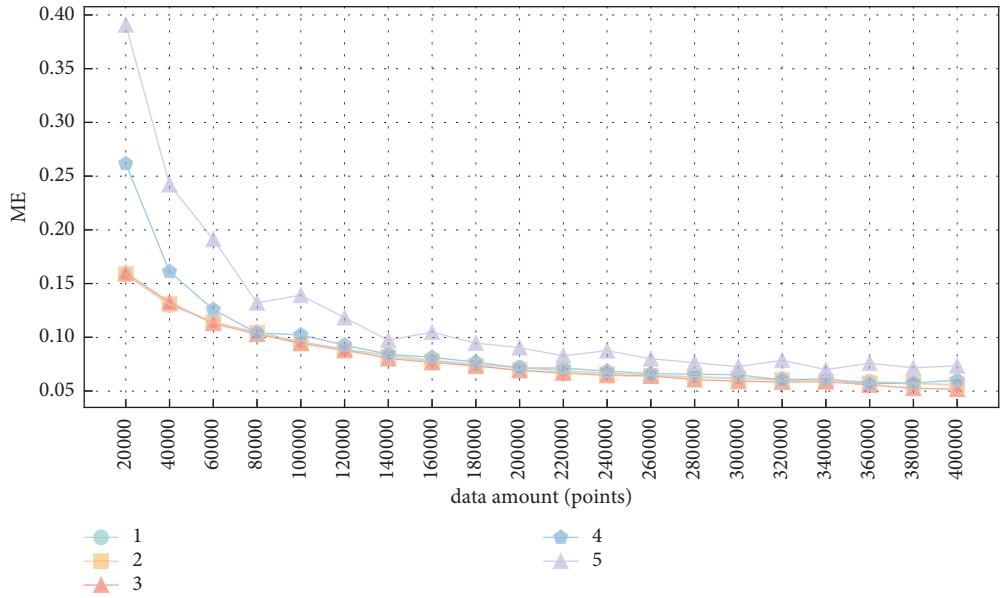

Figure 12: The estimation results for segments with different lengths.

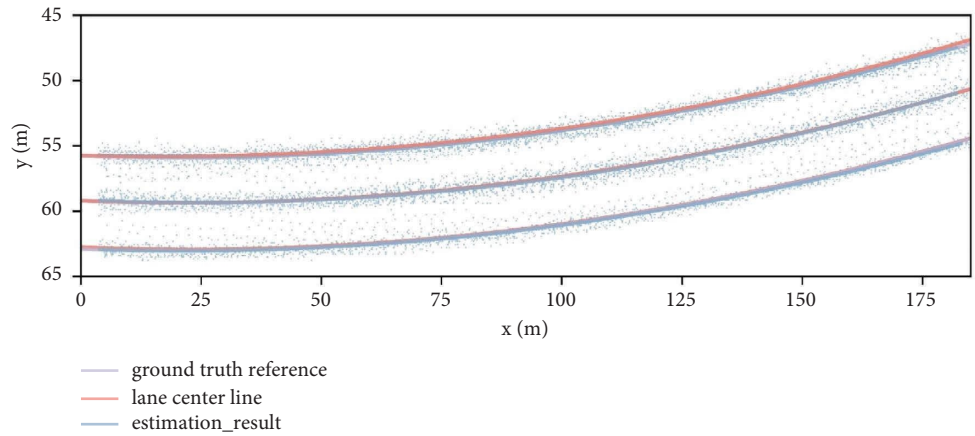

Figure 13: The estimation results based on the UAV trajectory data.

and management, their coverage and data size are limited by the resolution and size of the video. Previous studies have not been able to easily test or confirm their models on larger datasets [35]. To date, few studies have been published on the subject of long-wide trajectory data collection systems, particularly those that are environment-insensitive [9].

Table 3: The estimation results in different lanes based on the UAV trajectory data.

ME/(m)	Lane 1	Lane 2	Lane 3
ME of the ground truth reference and lane center lane	0.087	0.035	0.160
ME of the estimation result and ground truth reference	0.021	0.022	0.011
ME of the estimation result and lane center lane	0.064	0.067	0.182

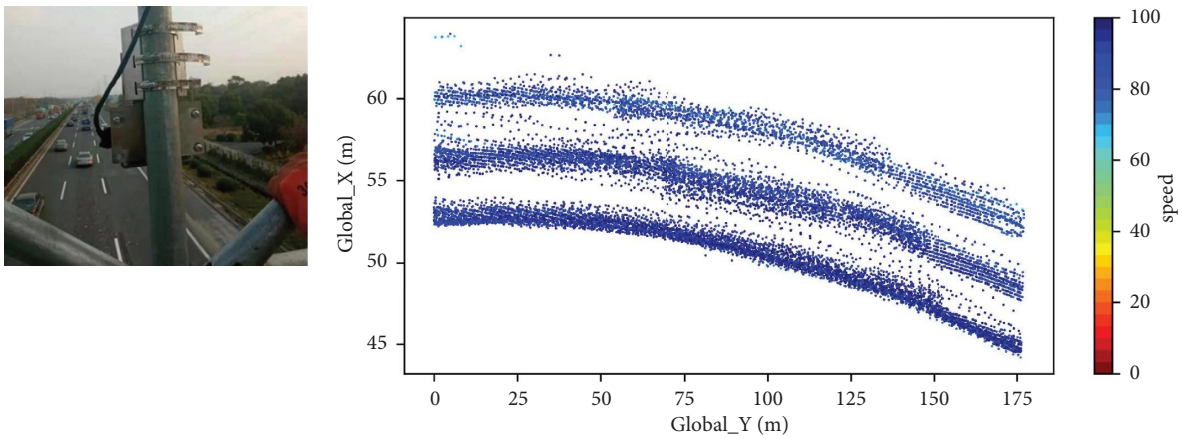

Figure 14: The MMW radar and the trajectory data. (a) The MMW radar installation position. (b) All trajectory points of the MMW radar.

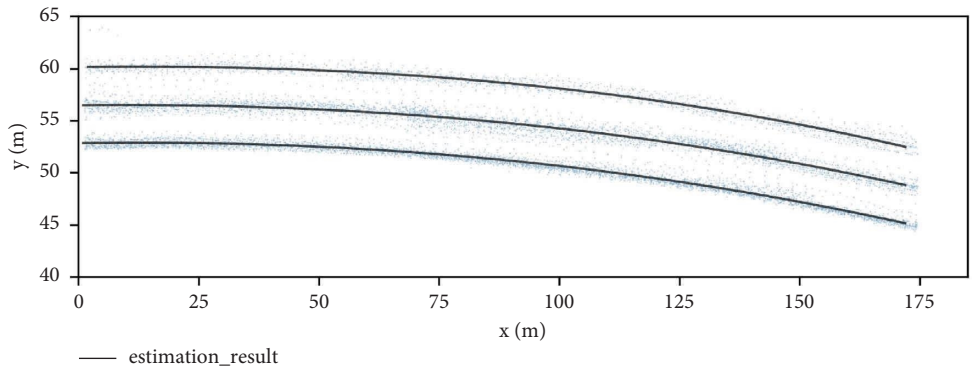

Figure 15: The estimation result of the MMW radar trajectory data.

Long-range millimeter-wave (MMW) radars have been recognized as having weak atmospheric attenuation and the ability to achieve over 200 meters of sensing and detection [36]. In this study, we apply the above method to the trajectory data of a MMW radar.

The trajectory data for this study was collected from an MMW radar installed 8 m above the Hangzhou Xifu Freeway, as shown in Figure 14(a). The radar system operates at 77 GHz and records vehicle location at a frequency of 10 Hz, with a maximum radar range of 250 m. Approximately, 10 minutes of radar data were collected and examined, with all trajectory points shown in Figure 14(b). The road segment has 3 lanes and 1 emergency lane, though the trajectory of the emergency lane was not collected in this study.

Based on the validation described above, the k-means method was chosen for clustering with a segmentation length of 3 m for around 10000 trajectory points. Since lane information is not available, the width of each lane is known to be 3.75 m. The ME value of the geometric estimation results for two adjacent lanes was evaluated based on whether it is close to 3.75 m.

As shown in Figure 15, the ME between the adjacent geometric estimation results is 3.61 and 3.75, respectively. While we do not have access to the actual lane widths for comparison, this result from our estimation method is very close to the expected lane widths. The effectiveness of the method has been demonstrated in previous sections, which increases our confidence in its application to pure trajectory data. It is reasonable to assume that the results of the estimation using millimeter-wave radar data are reliable.

6. Conclusion

In this paper, we presented a method for estimating lane-level geometry using trajectory data, which is based on the prior features of lateral and longitudinal of vehicle

trajectories without lane information. The choice of parameters in the method was determined through experiments in various scenarios, including different data amounts, segment lengths, lane change removal, and two clustering methods. The results of the manual calibration data showed that the method is effective after parameter selection. Based on these results, we can draw the following main conclusions:

(i) While the accuracy may not be high when the amount of data is small, it can still reach 0.1. When the data amount reaches a certain level, there is little improvement in fitting accuracy. Additionally, the ME is below 0.1 m when the number of trajectory points reaches an average of about 30 trajectory points per meter per segment.

(ii) Removing lane-changing data and using the k-medoids clustering method can slightly improve accuracy in the case of a large amount of data.

(iii) It is clear that the clustering algorithm will converge to a local optimum when the segmentation is too large. A segmentation of around 3 m (roughly the same as the lane width) is more appropriate.

(iv) The mean of vehicle trajectory lateral distribution may deviate from the center of the lane for various reasons, such as the innermost lane in the UAV data and lanes close to the ramp in the NGSIM I80 data, resulting in lower accuracy of lane-level geometry estimation.

As the main contribution of this study, we provide a method for estimating lane-level geometry using trajectory data from any sensor without the need for road information. This method can also be used for automated calibration caused by sensor offset under different conditions. The case study of MMW radar trajectory data is also demonstrated, though it would be more meaningful if the results could be compared to actual ground truth. Additionally, there has been no detailed analysis of the potential error patterns that may arise due to the offset caused by the clustering assumption. The current study is limited by the amount of microscopic trajectory data with lane line information and cannot be verified on a larger scale. In the future, we plan to conduct experiments under different road alignments and estimate road scenes with cross-section changes, such as ramps and bus stops. We also plan to investigate the performance of this method under different conditions and explore its potential use in information completion methods for fusion systems. However, our current knowledge of the characteristics of different lane and vehicle type trajectory lateral distributions is not sufficient to be used in this study.

Data Availability

The trajectory data used to support the findings of this study are available from the corresponding author upon request.

Conflicts of Interest

The authors declare that they have no conflicts of interest.

Acknowledgments

This study was jointly supported by the National Key R&D Program of China (2019YFB1600703), the Chinese National Natural Science Foundation (52172348 and 72001161), Research Project of Shanghai Science and Technology Commission (21XD1424100), the Shanghai Municipal Science and Technology Major Project (2021SHZDZX0100), and the Shanghai Municipal Commission of Science and Technology Project (19511132101).

References

[1] T. Fu, J. Stipancic, S. Zangenehpour, L. Miranda-Moreno, and N. Saunier, "Automatic traffic data collection under varying lighting and temperature conditions in multimodal environments: thermal versus visible spectrum video-based systems," *Journal of Advanced Transportation*, vol. 2017, Article ID 5142732, 15 pages, 2017.

[2] B. Maurin, O. Masoud, and N. P. Papanikolopoulos, "Tracking all traffic: computer vision algorithms for monitoring vehicles, individuals, and crowds," *IEEE Robotics and Automation Magazine*, vol. 12, no. 1, pp. 29–36, 2005.

[3] H. Liu, K. Teng, L. Rai, Y. Zhang, and S. Wang, "A two-step abnormal data analysis and processing method for millimetre-wave radar in traffic flow detection applications," *IET Intelligent Transport Systems*, vol. 15, no. 5, pp. 671–682, 2021.

[4] H. Liu, N. Li, D. Guan, and L. Rai, "Data feature analysis of non-scanning multi target millimeter-wave radar in traffic flow detection applications," *Sensors*, vol. 18, no. 9, p. 2756, 2018.

[5] J. Chen, S. Tian, H. Xu, R. Yue, Y. Sun, and Y. Cui, "Architecture of vehicle trajectories extraction with roadside LiDAR serving connected vehicles," *IEEE Access*, vol. 7, pp. 100406–100415, 2019.

[6] J. Wu, H. Xu, Y. Zheng, and Z. Tian, "A novel method of vehicle-pedestrian near-crash identification with roadside LiDAR data," *Accident Analysis & Prevention*, vol. 121, pp. 238–249, 2018.

[7] Fhwa, "Next generation simulation (NGSIM) vehicle trajectories and supporting data," 2006, https://ops.fhwa.dot.gov/trafficanalysistools/ngsim.html.

[8] R. Krajewski, J. Bock, L. Kloeker, and L. Eckstein, "The highd dataset: a drone dataset of naturalistic vehicle trajectories on German highways for validation of highly automated driving systems," in *Proceedings of the 2018 21st International Conference on Intelligent Transportation Systems (ITSC)*, pp. 2118–2125, IEEE, Maui, HI, USA, November 2018.

[9] J. Wang, T. Fu, J. Xue et al., "Realtime wide-area vehicle trajectory tracking using millimeter-wave radar sensors and the open TJRD TS dataset," *International Journal of Transportation Science and Technology*, vol. 12, no. 1, pp. 273–290, 2023.

[10] Q. Q. Shangguan, J. H. Wang, T. Fu, and S. E. Fang, "Quantification of cut-in risk and analysis of its influencing factors: a study using random parameters ordered probit model," *Journal of Transportation Safety & Security*, vol. 14, no. 12, pp. 2029–2054, 2021.

[11] Y. Du, B. Qin, C. Zhao, Y. Zhu, J. Cao, and Y. Ji, "A novel spatio-temporal synchronization method of roadside asynchronous MMW radar-camera for sensor fusion," *IEEE Transactions on Intelligent Transportation Systems*, vol. 23, no. 11, pp. 22278–22289, 2022.

[12] X. Chen, Z. Li, Y. Yang, L. Qi, and R. Ke, "High-resolution vehicle trajectory extraction and denoising from aerial videos," *IEEE Transactions on Intelligent Transportation Systems*, vol. 22, no. 5, pp. 3190–3202, 2021.

[13] P. Lindner, E. Richter, G. Wanielik, K. Takagi, and A. Isogai, "Multi-channel lidar processing for lane detection and estimation," in *Proceedings of the 2009 12th International IEEE Conference on Intelligent Transportation Systems*, pp. 1–6, IEEE, Louis, MO, USA, October 2009.

[14] C. Lei, C. Zhao, Y. Ji, Y. Shen, and Y. Du, "Identifying and correcting the errors of vehicle trajectories from roadside millimetre-wave radars," *IET Intelligent Transport Systems*, vol. 17, no. 2, pp. 418–434, 2022.

[15] C. Zhang, J. Wei, A. S. Hu, and P. Fu, "A novel method for calibration and verification of roadside millimetre-wave radar," *IET Intelligent Transport Systems*, vol. 16, no. 3, pp. 408–419, 2022.

[16] G. Kaur and D. Kumar, "Lane detection techniques: a review," *International Journal of Computer Application*, vol. 112, no. 10, 2015.

[17] D. Liang, Y.-C. Guo, S.-K. Zhang, T.-J. Mu, and X. Huang, "Lane detection: a survey with new results," *Journal of Computer Science and Technology*, vol. 35, no. 3, pp. 493–505, 2020.

[18] Y. Zhang, "Road geometry estimation using vehicle trails: a linear mixed model approach," *Journal of Intelligent Transportation Systems*, vol. 27, pp. 127–144, 2021.

[19] A. Eidehall, J. Pohl, and F. Gustafsson, "Joint road geometry estimation and vehicle tracking," *Control Engineering Practice*, vol. 15, no. 12, pp. 1484–1494, 2007.

[20] A. Bar Hillel, R. Lerner, D. Levi, and G. Raz, "Recent progress in road and lane detection: a survey," *Machine Vision and Applications*, vol. 25, no. 3, pp. 727–745, 2014.

[21] Z. Kim, "Robust lane detection and tracking in challenging scenarios," *IEEE Transactions on Intelligent Transportation Systems*, vol. 9, no. 1, pp. 16–26, 2008.

[22] J. Jung and S.-H. Bae, "Real-time road lane detection in urban areas using LiDAR data," *Electronics*, vol. 7, no. 11, p. 276, 2018.

[23] X. Tang, Z. Zhang, and Y. Qin, "On-road object detection and tracking based on radar and vision fusion: a review," *IEEE Intelligent Transportation Systems Magazine*, vol. 14, no. 5, pp. 103–128, 2022.

[24] Y. Liu and Y. Liu, "A data fusion model for millimeter-wave radar and vision sensor in advanced driving assistance system," *International Journal of Automotive Technology*, vol. 22, no. 6, pp. 1695–1709, 2021.

[25] C. Cao, J. Gao, and Y. C. Liu, "Research on space fusion method of millimeter wave radar and vision sensor," *Procedia Computer Science*, vol. 166, pp. 68–72, 2020.

[26] Q. Lu, R. Wang, B. Yang, and Z. Wang, "Trajectory splicing," *Knowledge and Information Systems*, vol. 62, no. 4, pp. 1279–1312, 2020.

[27] M. Nikodem, M. Słabicki, T. Surmacz, P. Mrówka, and C. Dołęga, "Multi-camera vehicle tracking using edge computing and low-power communication," *Sensors*, vol. 20, no. 11, p. 3334, 2020.

[28] W. Li, Y. Guan, L. Chen, and L. Sun, "Millimeter-wave radar and machine vision-based lane recognition," *International Journal of Pattern Recognition and Artificial Intelligence*, vol. 32, no. 05, Article ID 1850015, 2018.

[29] Á. F. García-Fernández, L. Hammarstrand, M. Fatemi, and L. Svensson, "Bayesian road estimation using onboard sensors," *IEEE Transactions on Intelligent Transportation Systems*, vol. 15, no. 4, pp. 1676–1689, 2014.

[30] L. Hammarstrand, M. Fatemi, Á. F. García-Fernández, and L. Svensson, "Long-range road geometry estimation using moving vehicles and roadside observations," *IEEE Transactions on Intelligent Transportation Systems*, vol. 17, no. 8, pp. 2144–2158, 2016.

[31] L. Liu and L. Sun, "Research on wheelpath lateral distribution for freeway asphalt pavements," *Tongji Daxue Xuebao/Journal of Tongji University(Natural Science)(China)*, vol. 33, no. 11, pp. 1449–1452, 2005.

[32] H. Huang and C. Jianchuan, "Operation characteristics of vehicles in straight section of urban arterial road based on drone technique," *Journal of Transport Information and Safety*, vol. 37, no. 3, pp. 51–60, 2019.

[33] J. Xu, X. Luo, and Y.-M. Shao, "Vehicle trajectory at curved sections of two-lane mountain roads: a field study under natural driving conditions," *European Transport Research Review*, vol. 10, no. 1, pp. 12–16, 2018.

[34] P. Spacek, "Track behavior in curve areas: attempt at typology," *Journal of Transportation Engineering*, vol. 131, no. 9, pp. 669–676, 2005.

[35] X. Zhang, J. Sun, X. Qi, and J. Sun, "Simultaneous modeling of car-following and lane-changing behaviors using deep learning," *Transportation Research Part C: Emerging Technologies*, vol. 104, pp. 287–304, 2019.

[36] A. Kiitayama, A. Kuriyama, H. Kagaishi, and H. Kuroda, "High-density implementation techniques for long-range radar using horn and lens antennas," *IEICE- Transactions on Electronics*, vol. 104, no. 10, pp. 596–604, 2021.